Simulation study for vibration reduction in a high-precision dual gantry system

Marco Astner, Franz-Josef Falkner (supervisor)

***Abstract*—This master thesis investigates the application of active vibration isolation systems for a high-precision dual gantry system used in the semiconductor industry. Two beams are used in the dual gantry, and a tool is on top of either beam.**
A flexible multi-body digital twin is modeled with experimental data to achieve high-fidelity simulation. Linear motors with a modeled motor driver and springs and dampers from a modal analysis improve the accuracy of the digital twin.
The dual gantry encounters two primary vibration sources: environmental disturbances and the drive forces generated by the movement of either tool or beam.
The content of this thesis contributes to the evolution of vibration isolation technology in the semiconductor manufacturing industry by developing a system that offers an actuator block with a controller. Central to this block are four isolators, eight actuators, and six sensors. The software is fully parameterized for a given machine model, and design considerations can be accessed through comparative data.
The key performance aspect of the implemented tuning algorithms is decreasing the vibration amplitudes at the tooltip and increasing the machine's output. A combination of feedforward control algorithms with parasitic effects and a multidimensional feedback controller with an analysis of sensor types and structures achieves a vibration reduction of $99.9\,\%$.

***Index Terms*—active vibration isolation, feedforward control, inertial sensors, adaptive tuning, MIMO feedback, floor stiffness, and linear motor control.**

I. Introduction

THE study of vibrations and their applications has a rich history, dating back to the fifth century BC when the Pythagoreans first associated vibrations with the theory of music and the theory of acoustics [1]. The exploration of vibrations continued with chapter VII of [2] as Galileo's study of the small oscillations of a pendulum in 1632. This foundational work paved the way for further investigations like the vibrations of a stretched cord by Brook Taylor, D'Alembert, Euler, and Daniel Bernoulli in the first half of the eighteenth century. In terms of the finite amplitude of vibrations, Euler first studied them in 1736. [2]
Applications of passive vibration isolation system (PVIS) started in the aircraft industry in the 1950s due to mechanical failure at random vibrations [3]. Essential components are resilient, load-supporting, energy-dissipating parts, typically made from metal, pneumatic elements, wire mesh, or elastomer. Alternatives can be air cushions or similar.
During displacement, the spring's opposing force creates a resonance that can amplify vibrations. This leads to limited effectiveness at lower frequencies and an inability to adapt to changing vibration patterns. [4]
In the 1960s, control engineers advanced with the first principles of active vibration isolation system (AVIS) and, in addition, so-called skyhook damping [5]. These innovations have been particularly beneficial for seismic isolation platforms for manufacturing processes and automotive suspensions.
The need for active vibration isolation system (AVIS) is particularly acute in the semiconductor industry. Precision and stability are paramount in this field, particularly in processes such as lithography and inspection, which usually involve the position of a

F-J. Falkner is with the Department of Mechatronics, Innsbruck, Austria, e-mail: franz-josef.falkner@mci.edu.

silicon wafer relative to an optical setup at a fast-moving stage. In these processes, even the slightest vibration can lead to significant defects and reduced yields. Precision and stability are paramount in this field.
Especially as Moore's law, which states that the number of transistors in an integrated circuit (IC) doubles about every two years, is slowly coming to an end. This happens due to physical, material, and electrical limitations. One solution would be transitioning from Moore's law of integrated circuit (IC) to Moore's Law of Packaging (MLP). [6]
Moore's Law of Packaging (MLP) represents the interconnection and integration of chips characterized by the highest transistor density, superior performance, and the lowest cost. Therefore, not transistors and their costs are essential for Moore's Law of Packaging (MLP), but the number of interconnections [6]. Consequently, the following algorithms are specially designed for machines in the packaging product group for the semiconductor industry, reducing vibration and increasing Units per Hour (UPH).
The remainder of this thesis is organized by Section II, which briefly introduces the theoretical background. Section III explains the methods used to design the needed algorithms for the control loops. Subsequently, Section IV presents the results and Section V concludes the thesis.

II. Theoretical background

Section II describes the basic control structure used in an active vibration isolation system (AVIS). Additionally, state-of-the-art control procedures and required sensor technology are described.

A. Vibration Isolation Systems

Reducing disturbances through vibrations in machinery is a topic of considerable interest in the academic world specializing in manufacturing. Initially, passive isolation systems are designed with a relatively low stiffness coefficient to resonate at frequencies lower than the standard excitation frequency [7]. In these systems, the spring is designed to isolate floor vibrations, and the damper is responsible for the resonant frequency. Adjusting the system's stiffness changes the resonance frequency, but the overshoot is to be controlled by a form of damping [8]. Passive systems must be designed for an inherent trade-off between poor high-frequency isolation and amplification of the resonance frequency [9]. In addition, robustness to external forces in the form of compliance is an issue. [8]
The combination of passive and active elements in parallel is shown in [10] as the most helpful solution for force control compared to similar structures. The following approach allows for control of peaks at the resonance frequency without severely impacting high-frequency performance [9]. Essentially, the passive damper is replaced by a combination of a sensor, measuring vibrations, and an active damper, such as a linear motor.

B. Control algorithms for vibration reduction

The concepts are illustrated within the comprehensive control strategy in Fig. 1. As can be seen, to achieve no change of position in the granite, the two mentioned algorithms of feedforward and feedback must be employed. In literature, the feedforward algorithm is also called Feedforward Control (FFC), as it mainly works against the movement of the beam, tool, etc., while the feedback algorithm, known as Feedback Control (FBC), primarily mitigates against floor vibrations and similar disturbances.

For the feedforward component, as the force command is predetermined, the motion controller provides the required trajectory. If the information is derived from the encoder level, an unstable feedback loop can result.
Studies have also explored possibilities for feedback control with a transformation from a multi-input multi-output (MIMO) to a single-input single-output

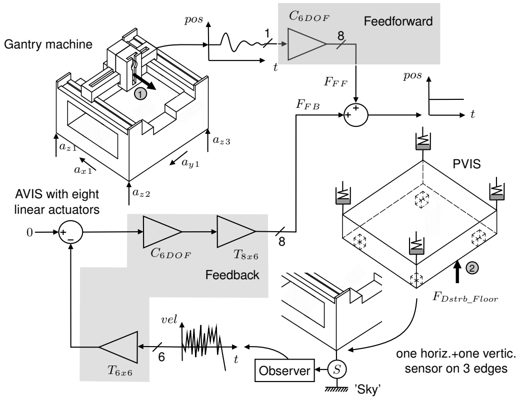

Fig. 1: Schematic of basic active vibration isolation system (AVIS) control structure

(SISO) system, as this is also visible in Fig. 1.
The controller can utilize this feedback algorithm either by using a proportional term for an impact on the resonance frequency, the derivative term creates a damping force and the integral term removes drifts of the payload [8]. Also, velocity feedback for so-called $Skyhook - damping$ is illustrated in [8], highlighting its advantages.
It is crucial to differentiate between applications where either vibrations or settling is critical. Lower gains are necessary to improve settling, though this compromises isolation performance.
Optimized pole locations for enhancing stability in the context of feedback control with high loop gains and low noise inertial sensors are applied in various cases, as well as an adaptive linear quadratic regulator (LQR) control scheme for significant attenuation of vibration isolations along with H_∞ methods.
The Kalman filter can be used to gather the necessary velocity for the feedback control loop. The data is smoothed for a more stable response.
Furthermore, the performance of the control structure depends on a detailed model of the actuator used, particularly regarding stroke, linearity, force generation, and the corresponding force constant.

C. Sensor technology

Considering feedback control, the sensor type significantly impacts the control structure's performance. Various inertial sensors have been compared by [11] for structural vibration control. The two main characteristics to distinguish between relative, inertial, and force sensors are transmissibility, which is the relation of the movement of granite to the floor at an infinite gain G, and compliance, which is a relation between the movement of the granite and the disturbance forces if the gain is infinitely high. The transmissibility should be as low as possible to reduce vibrations, and the compliance should be as low as possible to achieve the desired position by adapting to external forces. [8]
The advantages in terms of transmissibility and compliance of the inertial sensor can be shown. US patent [12] shows various details on the principle of inertial sensors. Geophones and position-based inertial sensors operate in the desired frequency range. In addition, the dynamic range of a position-based inertial sensor is generally superior to that of a geophone. In addition, the resolution of position-based inertial sensors is increased compared to geophones. [13]

III. Methods

A. Machine model

A detailed machine model is required to validate the designed algorithms for an active vibration isolation system (AVIS).
To fully integrate the machine in a working model, 57 Degree of Freedom (DOF) are defined. This structure is depicted in Fig. 2. The joints are represented as coordinate frames for the corresponding Degree of Freedom (DOF). The chosen software is Matlab Simscape.

B. Motor control

To drive the used linear actuators for the dual gantry machine and the eight actuators, a model

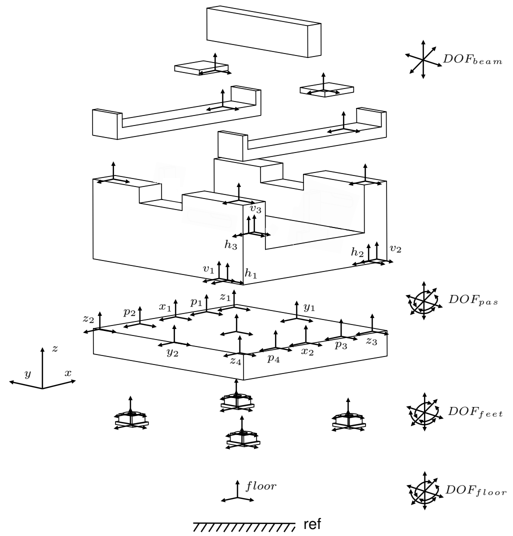

Fig. 2: Explosion schematic showing main frames and 57 Degree of Freedom (DOF) of the model

of the motor controller is needed in the form of a cascaded control structure of position and current control with an estimation of the velocity.
The desired trajectory acts as an input source for the position loop and is calculated as a planned S-curve trajectory with an adjustable a_{max}, v_{max}, p_{max}, and jerk time.

C. Optimal Feedforward Control (FFC)

The first approach for controlling the excitation by the gantry system is an optimal representation of the machine. The boundary conditions for Fig. 3 are that solely the beam undergoes movement along the x-direction, with the stator and the moving part of the linear motor being characterized by infinite damping and zero stiffness to ensure a rigid connection for the optimal case.
The set of Eqn. (1) can be derived to distribute the forces applied at the top of the machine to its eight linear actuators.

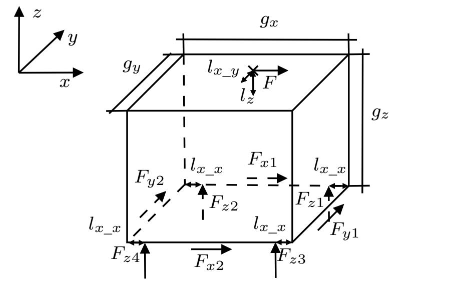

Fig. 3: Schematic drawing of the feedforward control strategy in the x-direction

$$
\begin{aligned}
&\text{I: } F_{x1} = F_{x2} = -\frac{F}{2} \\
&\text{II: } F_{z1} = \frac{Fg_z + Fl_z}{4\left(\frac{g_x}{2} - l_{x\_x}\right)} && \text{with: } F_{z1} = \frac{F_{z1,3}}{2} \\
& && F_{z2,4} = -F_{z1,3} \\
&\text{III: } F_{y1} = \frac{Fl_{x\_y}}{g_x} && \text{with: } F_{y2} = -F_{y1}
\end{aligned}
\tag{1}
$$

D. Beam excited Feedforward Control (FFC)

As the following iterative procedure for a more realistic machine model, the excitation of the gantry system comes directly from a beam. This leads to additional changes in the Center of Gravity (COG). Furthermore, the force applied at the top of the machine needs to be modeled due to friction losses between the beam and the primary granite. This is achieved by modeling the friction, for example, in the x-direction as a mass-spring-damper representation and deriving the force at the top of the granite through a state-space model. Afterward, the set of Eqn. (1) from Subsec. III-C can be used. The model is illustrated in Fig. 4, leading to the set of Eqn. (2).

$$
\begin{aligned}
\text{I: } m_1\ddot{x}_1 &= -d_1\dot{x}_1 + d_2(\dot{x}_2 - \dot{x}_1) + \\
&\quad - k_1x_1 - F_{beam} + F_{FF} \\
\text{II: } m_2\ddot{x}_2 &= -d_2(\dot{x}_2 - \dot{x}_1) + F_{beam}
\end{aligned}
\tag{2}
$$

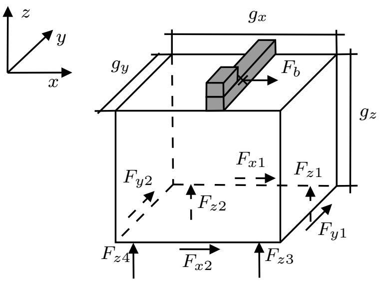

Fig. 4: Schematic drawing of the feedforward control strategy in the x-direction for a beam excited motion

E. Parasitic Feedforward Control (FFC)

Additional parasitic effects, such as those from the feet or the floor acting as a coupled mass, induce extra vibrations and must be considered. The primary issue for this problem can be described as a loss of actuator energy due to the fact that the linear actuator is placed on a parasitic mass rather than absolute ground.
A model illustrating this problem is shown in Fig. 5

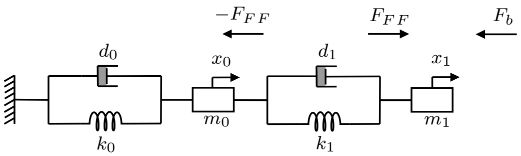

Fig. 5: Schematical concept of the FF optimization

Eqn. (3) shows a function derived from the state-space model depicted in Fig. 5. It reveals a factor needed as additional input over time to compensate for the loss of force from the missing absolute ground of the linear actuators.

$$f = \frac{-(F_b(k_0 + k_1 + sb_0 + sb_1 + s^2 m_0))}{F_{FF}(m_0 s^2 + b_0 s + k_0)} \tag{3}$$

F. Absolute inertial sensor

Subsec. II-C distinguishes between the primary sensor types possible for an active vibration isolation system (AVIS). To measure, as a first step, the difference in position between the mass of the granite m_1 and the sensor mass m_s, the model is illustrated in Fig. 6. As visible, ks, ds are the internal leaf spring properties of the sensor, and $k1$, $d1$ are the spring properties of the active vibration isolation system (AVIS). The dashed line symbolises the measurement lineal of the optical encoder.

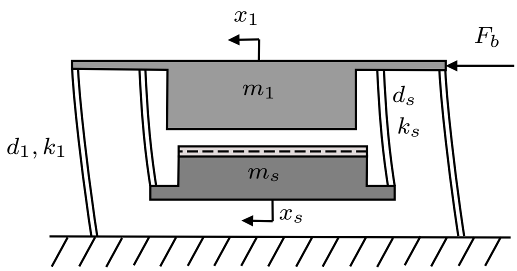

Fig. 6: Sensor principle of the absolute position measurement

From the representation in Fig. 6, the following state-space representation of

$$A = \begin{bmatrix} 0 & 1 & 0 & 0 \\ -\frac{k_s+k_1}{m_1} & -\frac{d_s+d_1}{m_1} & \frac{k_s}{m_1} & \frac{d_s}{m_1} \\ 0 & 0 & 0 & 1 \\ \frac{k_s}{m_s} & \frac{d_s}{m_s} & -\frac{k_s}{m_s} & -\frac{d_s}{m_s} \end{bmatrix} \tag{4}$$

is derived. The required velocity data is obtained by an observer structure with an observer gain of

$$L = q_0(\boldsymbol{A})\boldsymbol{N}^{-1} \begin{bmatrix} 0 & 0 & 0 & 1 \end{bmatrix}^T. \tag{5}$$

The absolute measurement of the sensor is visible in Fig. 7 at specific frequencies and applied in addition to a biquad filter for a higher dynamic range. The actual values on the axis are disabled

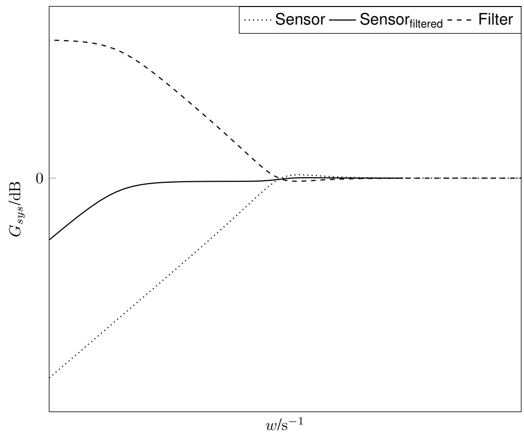

Fig. 7: Magnitude velocity plot of different sensor models

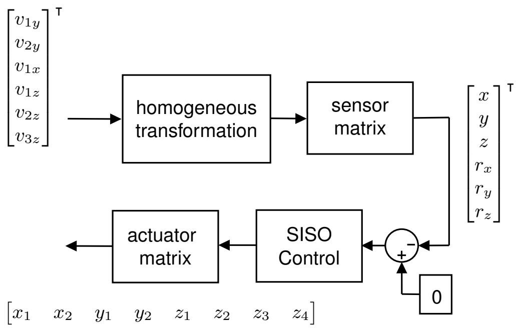

Fig. 8: Concept of feedback control based on multi-input multi-output (MIMO) to single-input single-output (SISO) conversion

since normalization for protecting particular details is not feasible with the known $0\,\mathrm{dB}$ and the frequency range for one decade.

G. Feedback Control (FBC)

The algorithm for Feedback Control (FBC) controls the disturbances acting on the granite by fusing the sensor data to a defined central point at the bottom of the granite. Therefore, the control algorithm can again be adjusted for a single-input single-output (SISO) system.
Afterward, the defined commands are distributed to the eight actuators.
Fig. 8 shows this basic procedure with an input of the six sensor data, the output of eight actuator currents for the linear motors, and the set-point of zero velocity after the calculation to a general coordinate for control.

H. Adaptive tuning

Four algorithms are designed to improve the simulation to the scenarios provided by the real world. The tuning of the force constant of the motor is done by measurements of the angular velocity around the z-axis for the x-direction actuators, followed by similar measurements for the y-direction actuators.
The underlying concept of this algorithm is that there should be no angular velocity around the z-direction if the motor constants are realistic to the real world and the actuators, in, for example, the x-direction, apply force in the same absolute direction.
A leveling algorithm improves the sensor model in Fig. 6 to measure static angles and compensate for unevenly distributed masses in a static sense.
The following algorithm is depicted in Fig. 9 and shows the adaptations of the parameters needed for the algorithm of the Feedforward Control (FFC). This must be done since the exact values of a mass or distribution of masses are not precisely known in the real world.

In addition, the mentioned parasitic effects in Subsec. III-E can not be controlled by $100\,\%$ due to the cross-coupling impacts. These effects can be canceled by a complete representation of the 57DOF in the control algorithms, but as these algorithms need to be integrated into a motion controller, this

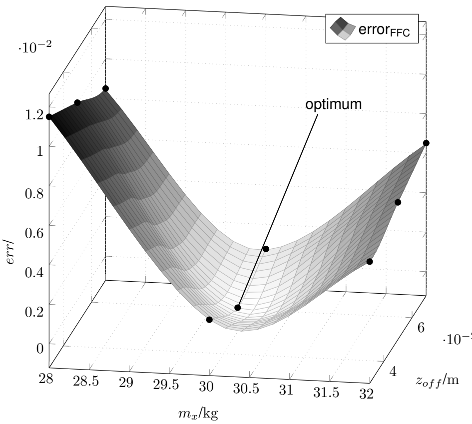

Fig. 9: Adaptive tuning of the feedforward control in the x direction for the mass in x as well as the COG in z of the beam

is not practical. Fig. 10 shows a slight change in the algorithm by adaptive tuning via a PI controller.

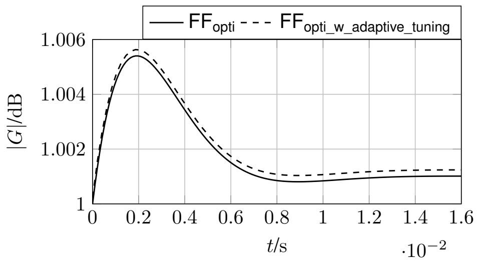

Fig. 10: Adaption of the time-depending factor due to cross-coupling effects

IV. Results and interpretation

Tab. I summarizes the critical outcome of this master's thesis. The following excitation is purely from gantry movement. No floor vibrations are applied. From top to bottom in Tab. I, only the passive vibration isolation system (PVIS) is applied. This is defined as a starting vibration level for analyzing the designed control algorithms.

Tab. I. Results for feedforward control, beam excited and parasitics

Description	contr. vibr. of m_1 in %
Beam excited	0 %
Beam excited + FFC	100 %
Beam excited + FFC + feet	99.87 %
Beam excited + FFC + feet + feet control	99.98 %
Beam excited + FFC + feet + feet control + adaptive tuning	99.994 %
Beam excited + FFC + feet + feet control + adaptive tuning + FBC	99.997 %

Without parasitic effects, like the feet or the floor in the machine model, the vibration control reaches a vibration reduction of 100 %. With additional parasitic effects, the vibration control is reduced due to the fact that the linear motor has no absolute ground reference.

With the defined algorithm from Subsec. III-E the vibration control is improved, with the adaptive tuning procedure and finally the Feedback Control (FBC). This feedback loop primarily affects the settling characteristic after a beam excitation and jitter improvements by damping the constant floor vibrations.

V. Conclusion

This master's thesis has thoroughly investigated the application of active vibration isolation systems for a high-precision dual gantry system used in the semiconductor industry. The critical procedures for developing an accurate digital representation of a specific production machine have been described, leading to the creation of a tuning algorithm tailored to meet the system's specific requirements.

A significant achievement of this research is the reduction of vibration amplitude at the machine's tool by 99.997 %, despite parasitic effects. The machine model demonstrated a high degree of accuracy compared to real-world data, and the adaptive tuning algorithms promise a certain customizability for deviations occurring in practical applications.

The implications of this thesis are particularly valuable in the early stages of developing new machine types. It addresses whether to use a combination of active vibration isolation system (AVIS) and passive vibration isolation system (PVIS) or rely on an utterly stiff system.

In the future, the designed algorithms must be applied on a real machine instead of a machine model. This thesis serves as the starting point for such a development process, detailing the main equations, potential integrations in motion controllers, and the system's boundaries.

ACKNOWLEDGMENT

I want to give special thanks to Besi Austria for providing the framework for this thesis and the MCI for being an inspiring place to conduct a master's program.

REFERENCES

[1] A. Dimarogonas, "The origins of vibration theory," *Journal of Sound and Vibration*, vol. 140, no. 2, pp. 181–189, 1990, https://doi.org/10.1016/0022-460X(90)90523-3.

[2] E. T. Whittaker, *A Treatise on the Analytical Dynamics of Particles and Rigid Bodies*. Cambridge: University Press, 1904.

[3] S. H. Crandall and W. D. Mark, "Random vibration in mechanical systems (second edition)," *Academic Press*, p. IV, 1963, https://doi.org/10.1016/B978-1-4832-3259-1.50002-2.

[4] C. Connolly, "Vibration isolation theory and practice," *Assembly Automation*, vol. 29, pp. 8–13, 02 2009, 10.1108/01445150910929802.

[5] D. Karnopp, "Active and Semi-Active Vibration Isolation," *Journal of Vibration and Acoustics*, vol. 117, no. B, pp. 177–185, 06 1995, 10.1115/1.2838660.

[6] R. R. Tummala, "Moore's law for packaging to replace moore's law for ics," in *2019 Pan Pacific Microelectronics Symposium (Pan Pacific)*, 2019, pp. 1–6, 10.23919/PanPacific.2019.8696409.

[7] M. H. Kim, H. Y. Kim, H. C. Kim, D. Ahn, and D.-G. Gweon, "Design and control of a 6-dof active vibration isolation system using a halbach magnet array," *IEEE/ASME Transactions on Mechatronics*, vol. 21, no. 4, pp. 2185–2196, 2016, doi: 10.1109/TMECH.2016.2539349.

[8] C. Collette, S. Janssens, and K. Artoos, "Review of active vibration isolation strategies," *Recent Patents on Mechanical Engineering*, vol. 4, no. 3, pp. 212–219, 2011, 10.2174/2212797611104030212.

[9] T. Muller, S. Hurlebaus, U. Stobener, and L. Gaul, "Modelling and control techniques of an active vibration isolation system," in *International Modal Analysis Conference IMAC XXIII*, 2005.

[10] C. C. Fuller, S. Elliott, and P. A. Nelson, *Active control of vibration*. Academic press, 1996.

[11] C. Collette, S. Janssens, P. Fernandez-Carmona, K. Artoos, M. Guinchard, C. Hauviller, and A. Preumont, "Review: Inertial Sensors for Low-Frequency Seismic Vibration Measurement," *Bulletin of the Seismological Society of America*, vol. 102, no. 4, pp. 1289–1300, 08 2012, 10.1785/0120110223.

[12] S. Manalis, "High-sensitivity interferometric accelerometer," 2002, U.S. Patent US6473187B1.

[13] C. Collette, S. Janssens, B. Mokrani, L. Fueyo-Roza, K. Artoos, M. Esposito, P. Fernandez-Carmona, M. Guinchard, and R. Leuxe, "Comparison of new absolute displacement sensors," *ISMA2012-USD2012*, pp. 1428–1434, uLB, Active Structures Laboratory, 50, av. F.D. Roosevelt, 1050, Brussels, Belgium, CERN, Engineering Department, 1211 Geneva 23, Switzerland.

Marco Astner is a student of the "Mechatronics & Smart Technologies" program at the MCI Innsbruck/Austria. In addition to his studies, he works as a control engineer at Ferchau Engineering. His primary focus is tuning machine axes' motion for the semiconductor industry.